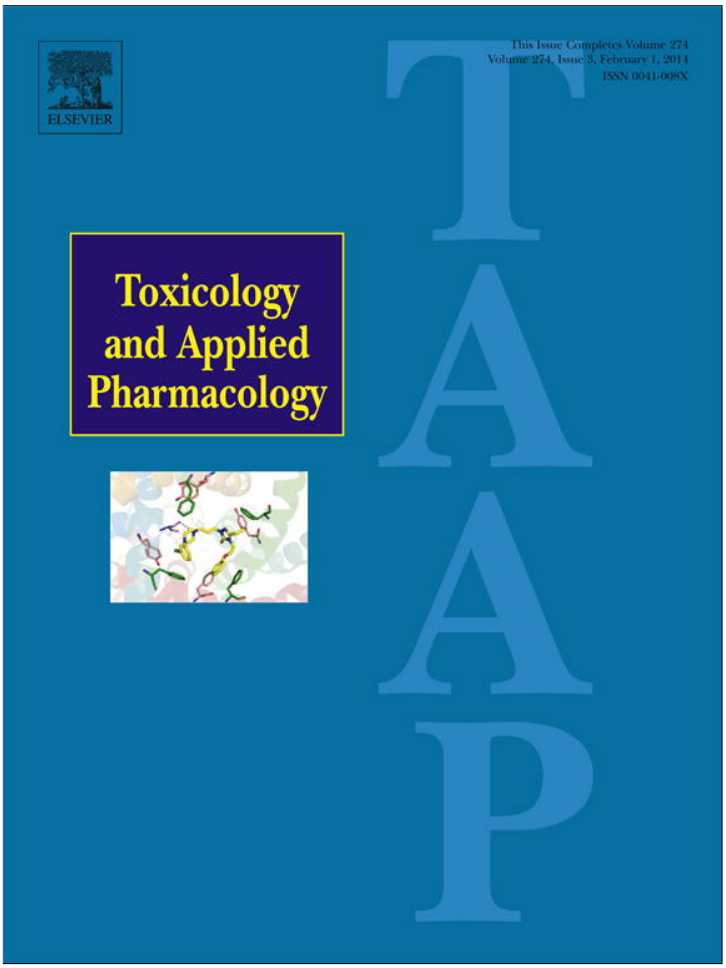

Toxicology and Applied Pharmacology 274 (2014) 471–479

Contents lists available at ScienceDirect

Toxicology and Applied Pharmacology

journal homepage: www.elsevier.com/locate/ytaap

Optimization of irinotecan chronotherapy with P-glycoprotein inhibition

Elisabeth Filipski [a,b], Elodie Berland [a,b], Narin Ozturk [a,b,d], Catherine Guettier [c], Gijsbertus T.J. van der Horst [e], Francis Lévi [a,b,c], Alper Okyar [a,b,d,*]

[a] INSERM, U776 "Rythmes biologiques et cancers", CAMPUS CNRS, 7 rue Guy Môquet, F-94801 Villejuif, France
[b] Univ Paris-Sud, UMR-S0776, Orsay F-91405, France
[c] Assistance Publique-Hôpitaux de Paris, Unité de Chronothérapie, Département de Cancérologie, Hôpital Paul Brousse, Villejuif F-94807, France
[d] Istanbul University Faculty of Pharmacy, Department of Pharmacology, Beyazit TR-34116, Istanbul, Turkey
[e] Department of Genetics, Erasmus University Medical Center, 3000 CA Rotterdam, the Netherlands

ARTICLE INFO

Article history:
Received 17 October 2013
Revised 17 December 2013
Accepted 19 December 2013
Available online 29 December 2013

Keywords:
Irinotecan
PSC833
Circadian rhythm
Cancer chronotherapy
P-glycoprotein

ABSTRACT

The relevance of P-glycoprotein (P-gp) for irinotecan chronopharmacology was investigated in female B6D2F$_1$ mice. A three-fold 24 h change in the mRNA expression of *Abcb1b* was demonstrated in ileum mucosa, with a maximum at Zeitgeber Time (ZT) 15 ($p < 0.001$). No rhythm was found for *abcb1a* in ileum mucosa, or for *Abcb1a/b* in Glasgow osteosarcoma (GOS), a mouse tumor cell line moderately sensitive to irinotecan. Non-tumor-bearing mice received irinotecan (50 mg/kg/day i.v. × 4 days) as a single agent or combined with P-gp inhibitor PSC833 (6.25 mg/kg/day i.p. × 4 days) at ZT3 or ZT15, respectively corresponding to the worst or the best irinotecan tolerability. Endpoints involved survival, body weight change and hematologic toxicity. Antitumor efficacy was studied in GOS-bearing mice receiving irinotecan (25, 30 or 40 mg/kg/day × 4 days) and +/− PSC833 at ZT3 or ZT15, with survival, body weight change, and tumor growth inhibition as endpoints. Non-tumor bearing mice lost an average of 17% or 9% of their body weight according to irinotecan administration at ZT3 or ZT15 respectively ($p < 0.001$). Dosing at ZT15 rather than ZT3 reduced mean leucopenia (9% vs 53%; $p < 0.001$). PSC833 aggravated irinotecan lethal toxicity from 4 to ~60%. In tumor-bearing mice, body weight loss was ~halved in the mice on irinotecan or irinotecan–PSC833 combination at ZT15 as compared to ZT3 ($p < 0.001$). PSC833–irinotecan at ZT15 increased tumor inhibition by ~40% as compared to irinotecan only at ZT15. In conclusion, P-gp was an important determinant of the circadian balance between toxicity and efficacy of irinotecan.

Introduction

The circadian timing of forty anticancer medications largely and predictably modified treatment tolerability and/or efficacy in experimental models. These findings led to the concept of chronotherapy through optimized circadian drug delivery (Lévi, 2006; Lévi and Okyar, 2011; Lévi et al., 2010). Improved outcomes on chronotherapy resulted from the circadian coordination of most determinants of drug effects, including the 24 h rhythmic changes in drug metabolism and detoxification, cell proliferation, DNA repair and apoptosis (Lévi and Okyar, 2011; Lévi et al., 2010). The clinical relevance of these findings was illustrated mostly in patients receiving oxaliplatin, 5-fluorouracil and leucovorin as first line treatment for metastatic colorectal cancer. Thus, tolerability was improved nearly 5-fold and antitumor activity was nearly doubled with a fixed chronotherapy schedule as compared to constant rate infusion (Lévi et al., 1997, 2007, 2008). A recent meta-analysis of three international randomized trials further revealed a statistically significant survival prolongation for men on this chronotherapy schedule as compared to conventional delivery, while the opposite was found for women (Giacchetti et al., 2012). The results supported sex-dependent differences in optimal chemotherapy timing and dose levels (Giacchetti et al., 2012; Lévi et al., 2007).

Irinotecan [7-ethyl-10-[4-(1-piperidino)-1-piperidino]-carbonyloxy-camptothecin] is a broadly used anticancer agent which is effective in patients with gastro-intestinal malignancies. The drug however triggered severe and unpredictable hematological, intestinal or systemic toxicities, which were detrimental to the patient quality of life, and impaired treatment safety and compliance (Innocenti and Ratain, 2003). Circadian timing profoundly altered irinotecan tolerability and antitumor efficacy. Notably, irinotecan dosing in the mid to late rest span (Zeitgeber Time, ZT7 to ZT11) proved to be least toxic and most effective in male ICR or male B6D2F$_1$ mice (Filipski et al., 2004; Granda et al., 2002; Ohdo et al., 1997). In contrast, the circadian times associated with the best and the worst tolerability in female B6D2F$_1$ were located in the first half of the dark span (ZT15) and in the early rest span (ZT3) respectively (Ahowesso et al., 2011; Li et al. 2013; Okyar et al., 2011). Irinotecan detoxification involves the active drug efflux from cells through ATP-binding cassette (ABC) transporters, especially P-glycoprotein (P-gp,

* Corresponding author at: Istanbul University, Faculty of Pharmacy, Department of Pharmacology, TR-34116 Beyazit, Istanbul, Turkey. Fax: +90 2125271825.
E-mail addresses: aokyar@istanbul.edu.tr, alper.okyar@inserm.fr (A. Okyar).

0041-008X/$ – see front matter © 2013 Elsevier Inc. All rights reserved.
http://dx.doi.org/10.1016/j.taap.2013.12.018

also designated as *abcb1a* and *abc1b* in mice and *ABCB1* in humans) and Multidrug Resistance Associated Protein 2 (MRP2, also designated as *Abcc2* in mice and *ABCC2* in humans). In prior work, we showed that *Abcc2* mRNA and protein expression patterns displayed robust circadian rhythms in mouse ileum mucosa that moderated irinotecan tolerability (Okyar et al., 2011).

P-gp was detected in many organs, yet its expression in liver and intestine played a critical role for irinotecan excretion and metabolism (Innocenti and Ratain, 2003). A few reports suggested a circadian regulation of P-gp in healthy mouse tissues. Thus, the mRNA expression of *Abcb1a* displayed a 24 h rhythm in total jejunum and liver of male C57BL/6J (Ando et al., 2005), in the liver of male C57BL/6 (Zhang et al., 2009) and in the ileum mucosa of male B6D2F$_1$ (Okyar et al., unpublished data). Moreover, circadian changes were recently demonstrated for the functional activity of P-gp in rat jejunum and ileum, with P-gp-dependent intestinal secretion being highest during the dark span as compared to the light span (Okyar et al., 2012). Recent articles further emphasized the occurrence of a control of efflux transporter gene expression by the molecular clock (Ballesta et al., 2011; Claudel et al., 2007; Gachon et al., 2006; Lévi and Schibler, 2007; Lévi et al., 2010). Convincing evidence was further offered regarding the molecular regulation of *Abcb1a* by clock-controlled transcription factors HLF and E4BP4 along the circadian time scale in the small intestine of male C57BL/6J mice (Murakami et al., 2008).

Here, the mRNA expression of P-gp was first determined in the ileum mucosa of female B6D2F$_1$ mice at ZT3 and ZT15 which in this mouse strain and gender corresponded to the best and the worst irinotecan tolerability, respectively (Ahowesso et al., 2011). P-gp mRNA expression was also assessed in early or late stage Glasgow osteosarcoma (GOS), following its inoculation to B6D2F$_1$ female mice. Indeed, GOS lacked coordinated molecular clocks at tumor tissue level following transplantation into male mice (Filipski et al., 2005). However a circadian rhythm in the mRNA expression of *ABCB1* was previously reported in synchronized and confluent human colorectal cancer (Caco-2) cells (Lévi et al., 2010). Thus, a possible circadian control of P-gp was here investigated in synchronized GOS cell cultures, using Per2::Luc GOS cells. GOS was chosen as a relevant tumor model, since it was initially used for probing the experimental activity of irinotecan (Bissery et al., 1996). This tumor displayed moderate circadian-dependent susceptibility to single agent irinotecan (Granda et al., 2002).

PSC833 (PSC), a second generation, a highly potent and selective inhibitor of P-gp in vitro (Johnson et al., 2003; Achira et al., 1999), ex vivo (Okyar et al., 2012), and in vivo (Kemper et al., 2003; Tai, 2000) was used as a pharmacological tool for probing the contribution of P-gp to irinotecan chronotherapy in female B6D2F$_1$ mice. PSC reverted the P-gp dependent multidrug resistance phenotype in several in vitro and in vivo tumor models (Cagliero et al., 2004; Krishna and Mayer, 1999; Page et al., 2000; Watanabe et al., 1995). However, the role of P-gp inhibitors as possible amplifiers of cancer chronotherapy has not yet been reported. PSC addition was first tested on irinotecan chronotoxicity in healthy mice. Systemic, bone marrow, ileum, colon and liver toxicities were evaluated. The relevance of dosing time, irinotecan dose and PSC addition were then assessed in mice with early stage GOS.

Materials and methods

Animals and circadian synchronization. The study was conducted in accordance with the guidelines approved for animal experimental procedures by the French Ethical Committee (decree 87-848). All the experiments involved female B6D2F$_1$ mice which were 7 weeks of age upon arrival from the breeder (Janvier, Le Genest St Isle, France). All the mice were housed under a 12/12 light/dark cycle in an autonomous chronobiological facility (Jouan-Thermo Electron LED S.A.S., Saint-Herblain, France) with food and water ad libitum for 3 weeks prior to any intervention. Each facility was equipped with temperature control (23 ± 1 °C) and comprised four or six compartments, each one being provided with separate filtered air (100 ± 10 l/min) and individual lighting regimen. Light intensity at cage level ranged from 220 to 315 lux. All the manipulations during the dark phase were performed under dim red light (7 lux).

Drugs. Irinotecan HCl (Chemos GmbH, Regenstauf-Germany) was diluted in sterile isotonic NaCl solution on each study day, prior to injections. The final drug solution was injected intravenously (i.v.) into the right retro-orbital venous sinus (Filipski et al., 2004). Irinotecan was administered once daily for 4 consecutive days (d1 to d4) at the ZT corresponding to the best or the worst tolerability, (i.e. ZT15 or ZT3) as established previously (Ahowesso et al., 2011; Okyar et al., 2011). Irinotecan doses ranged from 25 to 50 mg/kg/day according to experiment. PSC (a kind gift from P. Krajcsi, Solvo, Budapest, Hungary) was administered via intraperitoneal (i.p.) injection at a dose of 6.25 mg/kg/day for 4 days, 1 h before irinotecan injection. PSC dose was determined according to pervious study by Song et al. (1999) and based on our preliminary experiments.

Tumor model. Mouse GOS tumor cells were provided by the Research Center of Aventis Pharma (Vitry sur Seine, France). For the in vivo experiments, GOS fragments (~4 × 4 × 4 mm^3) were prepared following tumor excision from a donor mouse (Tampellini et al., 1998). One fragment was inoculated subcutaneously in each flank of female C57BL/6 mice aged 7 weeks.

For the in vitro experiments, the original GOS cell line was modified through stable introduction of a luciferase reporter gene under the control of the Per2 promoter (1.5 kb upstream of the ATG start codon and containing the important e-Box sequences).

Mouse Per2::Luc GOS cells were cultured in minimum essential medium alpha (MEMα, Invitrogen, France), supplemented with penicillin (100 U/l), streptomycin (100 μg/ml), glutamine (2 mM, Fischer Scientific, France) and 10% of fetal bovine serum (FBS) (Dutscher, France). The cells were maintained at 37 °C in a humidified atmosphere containing 5% CO_2. After one night incubation, cells were synchronized with 100 nM dexamethasone (Dex) (Sigma, Aldrich, France) dissolved in absolute ethanol (final ethanol concentration of 0.001%) for 2 h. The cells were then washed with 1 ml phosphate buffered saline (PBS) and the medium was replaced with a fresh one without Dex. Dex exposure onset was defined as Circadian Time 0 (CT0).

In order to identify any circadian pattern in clock gene *Per2* transcriptional activity, 3 × 10^4 GOS cells per 35-mm Petri dishes (one Petri dish for non-synchronized and three Petri dishes for synchronized cell populations) were seeded and incubated one night prior to the experiment. Before recording, cells were treated with Dex for 2 h. 0.1 μM luciferine (Promega, France) was added to the culture medium, upon completion of Dex exposure. Bioluminescence from each Petri dish was recorded as photon counts/s every 10 min for 96 h in a LumiCycle32 (Actimetrics, USA), a 32-channel automated luminometer placed within a 37 °C incubator in a temperature-controlled room.

Abcb1a and Abcb1b mRNA expression patterns in ileum mucosa and GOS. Ileum mucosa samples were removed immediately after euthanizing mice at ZT3 or ZT15, then frozen in liquid nitrogen and stored at −80 °C. *Abcb1a* and *Abcb1b* mRNA levels were measured by quantitative real time polymerase chain reaction (qRT-PCR).

P-gp expression was determined in GOS tumors by determining *Abcb1a* and *Abcb1b* mRNA expression levels. Tumors were sampled at ZT5 nine days after subcutaneous tumor inoculation at ZT3, and processed for qRT-PCR as above described.

Possibly rhythmic expression of *Abcb1a* and *Abcb1b* was further sought in synchronized cultures of proliferating Per2::Luc GOS cells. 9 × 10^4 cells per 60-mm Petri dish were seeded as previously described. Cells were scraped from three different Petri dishes in lysis solution solution (4 M guanosine isothiocyanate + 0.75 M sodium citrate + N-lauryl sarcosine 10% + 0.1 M β-mercaptoethanol) and frozen at

−80 °C every 4 h for 48 h. Total RNA was purified using the method of Chomczynski and Sacchi (2006) and stored at −80 °C until use.

PCR was performed with a LightCycler 480 (Roche, Meylan, France) using SYBR green I dye detection according to the manufacturer's recommendations. cDNA was added to a reaction mixture (Faststart DNA SYBR Green I; Roche Diagnostics, Meylan, France) with appropriate primers at 0.5 μM each. Relative mRNA abundance was calculated using a standard curve method. Expression levels were normalized to the levels of the constitutively and non-rhythmically expressed *36B4*. The following primers were used for *Abcb1a* (forward, 5′-CCA TGC TGA GAC AGG ATG TGA-3′ and reverse, 5′-TCC TGC TAT CGC AAT GAT GG-3′); for *Abcb1b*, (forward, 5′-CCA TGG CTG GAT CAG TGT TTC-3′ and reverse, 5′-CAG GCA GTG AGT CGA TGA AC-3′.); for *36B4*, forward 5′-GCT GAT GGG CAA GAA CAC CA-3′ and reverse 5′–CCC AAA GCC TGG AAG AAG GA-3′.

Circadian dependent toxicities of irinotecan as single agent or combined with PSC in healthy mice. A total of 60 mice received four consecutive daily injections of irinotecan (50 mg/kg/day on d1 to d4) with or without PSC (6.25 mg/kg/day), either at ZT3 or at ZT15. At each ZT, 12 mice received single agent irinotecan, and 12 mice received the drug combination. In addition, 3 mice received PSC only and 3 mice received vehicle only as controls for each ZT. Body weight and survival were recorded daily during 6 days. Body weight change was computed relative to its pretreatment value at the same ZT. This biomarker reliably evaluated circadian changes in the toxicity of several anticancer drugs, including irinotecan (Filipski et al., 2004; Ohdo et al., 1997).

Hematologic and intestinal toxicities. Right retro-orbital sinus blood was sampled on EDTA at ZT3 or ZT15 on d6, i.e. 2 days after irinotecan treatment completion. Circulating leukocytes and bone marrow nucleated cells were counted (Filipski et al., 2004). The upper femoral head, as well as a segment of ileum and colon and a liver lobe were sampled at ZT3 or ZT15, fixed, sliced and stained with hematoxylin–eosin (H&E) as described previously (Okyar et al., 2011). All tissue samples were examined by the same senior histopathologist. Bone marrow toxicity was graded as 0 (no lesion), 1 (congestion), 2 (mild cytopenia) and 3 (cellular necrosis). Ileum and colon mucosa lesions were graded as 0 (none), 1 (moderate) or 2 (severe).

Circadian dependent antitumor efficacy. A total of 84 mice were inoculated with a ~$4 \times 4 \times 4$ mm^3 subcutaneous GOS implant in each flank, using a 12-gauge trocar. The mice received irinotecan (25, 30 or 40 mg/kg/day for 4 days) starting 5 days after tumor inoculation (d5–8). Irinotecan was combined with PSC or not. There were 6 mice for each dose, administration time (ZT3 and ZT15) and treatment modality (single agent irinotecan or combined irinotecan–PSC). Six control mice in each ZT received vehicle with or without prior PSC. Mortality was recorded daily. Body weight was measured and tumor size was determined at the time of injection with a caliper during treatment (daily) and after (3 times a week) the treatment period. Tumor weights (mg) were estimated from two perpendicular measurements (mm), as described by Tampellini et al. (1998).

Statistical analyses. Means and SEM were calculated for each study variable. Differences in mRNA expression level of *Abcb1a* and *Abcb1b* according to ZTs and CTs were validated using analyses of variance (ANOVA). The statistical significance of a sinusoidal rhythm in mRNA expressions was further assessed with Cosinor analysis (De Prins and Hecquet, 1992). The input period was 24 h for those data obtained in mice synchronized with LD12:12, or the dominant period was computed with spectral analysis for the in vitro data as described below.

Bioluminescence time series were first imported into Lumicycle analysis program (Actimetrics, USA). Due to high initial transients of luminescence after medium change, the first 12 h of data was excluded from analysis. A linear baseline trend was subtracted from raw data (polynomial order = 1). Detrended data (counts/s) were plotted against time (h) in culture. The spectrum was determined by spectral analysis (FFT, Fast Fourier Transform) from the original signal for the non-synchronized cell culture dish, and for the three synchronized cell culture dishes. The corresponding period for the highest harmonic was computed, and used as input for Cosinor. The spectrum and corresponding period for the two apparent cycles were also determined for each cell culture dish in order to validate the dominant period according to all signals. This period was also used as an input one for Cosinor analysis of the in vitro *Abcb1a* and *Abcb1b* data.

Whenever the probability of the rejection of a non-null amplitude with Cosinor was <5%, this linear least squares method yielded the parameters of the fitted cosine function best approximating all data with their 95% confidence limits, including the mesor (rhythm-adjusted mean), the amplitude (half the difference between the minimum and the maximum of best-fitting cosine function), and the acrophase (Ø, time of maximum). Incidence data were compared by χ^2 test. All statistical tests were two-sided and performed using PASW Statistics 18 software (SPSS Inc. Chicago, IL).

Results

Gene and tissue specificity of circadian control of P-gp expression

Time dependent changes in P-gp mRNA expression were found in the ileum mucosa of female mice. GOS tumor expressed both isoforms of P-gp, i.e., *Abcb1a* and *Abcb1b*, following the subcutaneous tumor inoculation in mice.

Abcb1b expression displayed large and statistically significant threefold circadian changes in ileum mucosa (p from ANOVA = 0.03). Mean values were highest at ZT15 and lowest at ZT3. In contrast, no significant time-dependent variation was found for *Abcb1a* (p = 0.46) (Fig. 1). The mRNA expression of *Abcb1b* was several folds as high as that of *Abcb1a* both in ileum mucosa and in GOS tumor in vivo. Thus, the respective 24 h means of *Abcb1b* and *Abcb1a* mRNA expressions were 4.91 ± 1.18 and 2.41 ± 0.52 in the ileum mucosa (p from ANOVA = 0.06), and 3.17 ± 1.16 and 0.48 ± 0.04 in GOS tumors sampled at ZT5 ($p < 0.001$).

The possible circadian dependency of *Abcb1a* and *Abcb1b* in GOS cells (in vitro) was explored in dex-synchronized cultures of Per2::Luc GOS cells. First, a circadian rhythm with a dominant 28 h period was demonstrated with FFT of detrended data for Per2 bioluminescence in each of the three synchronized cell culture dishes. The three sinusoidal patterns were validated with cosinor ($p < 0.0001$), with similar acrophases clustered around CT3:50 modulo 28 h (Fig. 2, upper panel).

Despite the adequate circadian synchronization of Per2::luc GOS cells, no time dependency or rhythmic pattern was found for *Abcb1a*

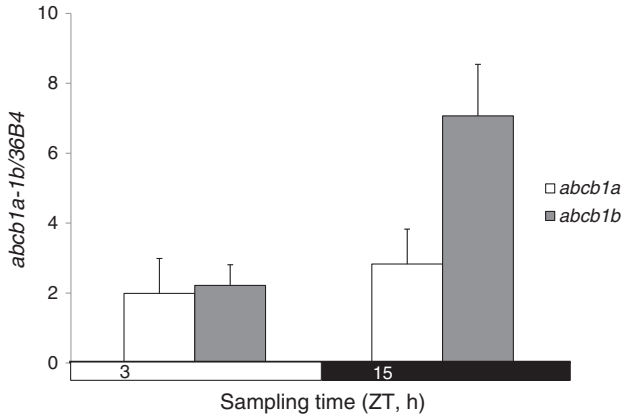

Fig. 1. Time-dependent mRNA expression of *Abcb1a* and *Abcb1b* in ileum mucosa of female B6D2F$_1$ mice. Mean ± SEM of data from 4 or 5 mice. *Abcb1b* mRNA expression was significantly higher at ZT15 as compared to ZT3 (ANOVA; p = 0.03).

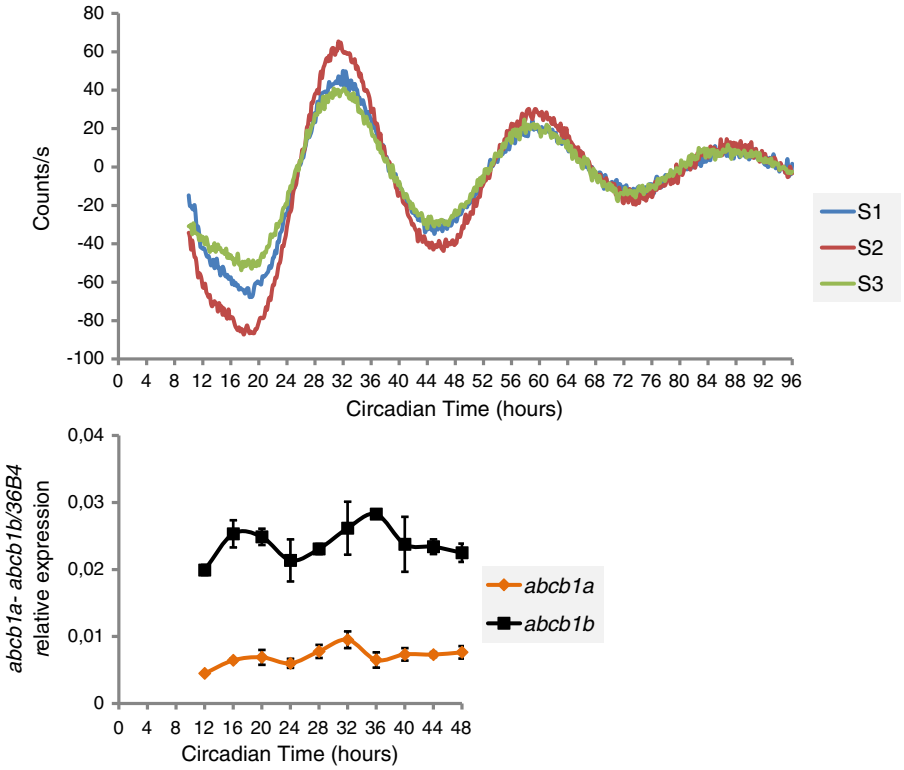

Fig. 2. Temporal changes in P-gp mRNA expression in dexamethasone-synchronized Per2::Luc GOS cell cultures. Upper panel: Bioluminescence patterns reflecting *Per2* transcriptional activity dynamics in three individual cell cultures (S1, S2 and S3). Photons from each cell culture were counted automatically every 10 min for 96 h. Circadian Time CT0 corresponded to the onset of dexamethasone 2 h exposure. Fast Fourier Transform identified a circadian rhythm with a dominant period $\tau = 28$ h which was statistically validated with cosinor ($p < 0.0001$) for S1, S2 and S3. Lower panel: Relative mRNA expression patterns of *Abcb1a* and *Abcb1b* in synchronized mouse Per2::Luc GOS cell cultures. Mean ± SEM of gene expression determined with qRT-PCR in three separate synchronized cell cultures sampled at the same CT (Total $n = 30$). No circadian rhythm was validated for *Abcb1a* or *Abcb1b* (cosinor with $\tau = 28$ h: $p = 0.53$ and $p = 0.48$, respectively).

and *Abcb1b* (Fig. 2, lower panel) (p from ANOVA = 0.32 and p = 0.402, respectively). No 28 h rhythm was detected either with cosinor (p = 0.53 and p = 0.48, respectively). However, consistent with the in vivo data the expression of *Abcb1b* was four-fold as high as that of *Abcb1a*.

Dosing time dependent tolerability of irinotecan with or without PSC in non-tumor bearing mice

Survival and body weight change

Irinotecan treatment (50 mg/kg/day) resulted in a single toxic death which occurred at ZT3 (1/24 mice, 4%). Mean body weight reached a nadir two days after treatment completion. Mean maximum body weight loss was 17% in the mice treated at ZT3 as compared to 9% in those dosed at ZT15 (p from ANOVA <0.001). PSC addition severely aggravated irinotecan-related mortality, which reached 66% for the mice treated at ZT3 (8/12) and 58% for those injected at ZT15 (7/12). PSC addition further ablated the dosing time dependency of irinotecan-induced body weight loss (Fig. 3).

Hematologic, intestinal and liver toxicities

Mean leukopenia worsened ~six-fold in the mice receiving irinotecan at ZT3 as compared to ZT15 (p = 0.001) (Fig. 4a). Similarly, the depletion in bone marrow nucleated cell count was ~three fold as large in the mice treated at ZT3 as compared to ZT15 (p < 0.001) (Fig. 4b). The combination of PSC and irinotecan decreased the mean counts in circulating leukocytes and those in bone marrow nucleated cells both at ZT3 and ZT15, without any statistically significant difference according to dosing time (p = 0.54). Thus PSC addition not only worsened irinotecan-induced hematological toxicities, but also suppressed their dosing time dependency. However, PSC833 alone increased circulating leukocyte counts both at ZT3 and ZT15 as compared to vehicle-treated mice. Histological analysis further revealed a ~three-fold increase in the occurrence of grade 2 or 3 lesions in femoral bone marrow in the mice on the PSC–irinotecan combination as compared to single agent irinotecan (7/9, 78% vs. 3/12, 25% respectively; p from $\chi^2 = 0.024$). In contrast, neither ileum nor colon histological toxicities were significantly modified with PSC addition. The incidence of grade 2 or 3 lesions in ileum mucosa ranged from 6/7 (86%) on single agent to 10/10 (100%) on the drug combination (p = 0.41). The respective

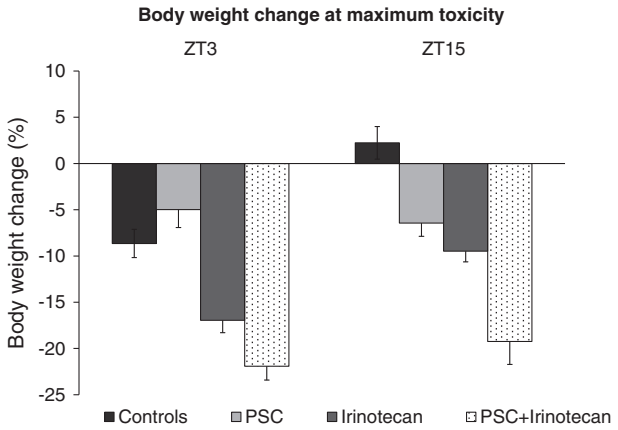

Fig. 3. Maximum body weight change as a function of irinotecan circadian timing. Data obtained two days after treatment completion are expressed as mean ± SEM relative to pre-treatment values. Body weight loss was significantly larger following treatment at ZT3 as compared to treatment at ZT15 for single agent irinotecan (ANOVA, p = 0.001), but not for the combination of irinotecan and PSC (ANOVA, p = 0.37).

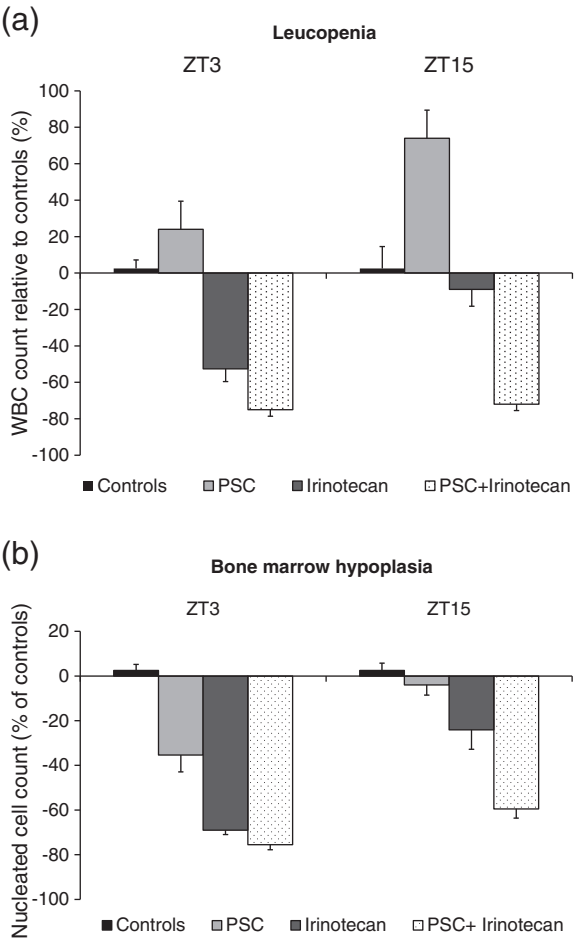

Fig. 4. Time dependent toxicity of irinotecan as a single agent or in combination with PSC. Data obtained at maximum toxicity i.e. two days after treatment completion. All data are expressed as mean ± SEM. (a) Leucopenia. Hematological toxicity was significantly larger following treatment at ZT3 as compared to ZT15 for single agent irinotecan (ANOVA, $p = 0.001$) but not for the combination of irinotecan and PSC (ANOVA, $p = 0.54$). (b) Bone marrow hypoplasia. The count in nucleated bone marrow cells was significantly less following treatment at ZT3 as compared to ZT15 for single agent irinotecan as well as for the combination of irinotecan and PSC (ANOVA, $p = 0.001$ and $p = 0.016$, respectively).

figures in colon mucosa were 1/7 (14%) and 6/11 (55%) ($p = 0.11$). No histological lesion was documented in liver.

Dosing time dependent therapeutic effects of irinotecan in tumor-bearing mice

Irrespective of dosing time, the mortality rates of mice on single agent irinotecan ranged from 17% (25 mg/kg/day) to 8% (30 mg/kg/day) and 25% (40 mg/kg/day) (χ^2, $p = 0.5$). The corresponding rates for the combination of irinotecan and PSC were 8%, 8% and 50% (χ^2, $p = 0.01$). This finding supported the consideration of both lower dose levels as therapeutic ones in this model. Mice lost significantly less body weight following treatment at ZT15 as compared to ZT3, both on single agent and on combined therapy (p from ANOVA, $p < 0.001$) (Fig. 5). No statistically significant differences were found for body weight changes according to irinotecan dose level ($p = 0.3$), within the dose range tested.

PSC accelerated tumor progression as compared to untreated controls both at ZT3 and ZT15 (Figs. 6a, b and c). However this effect of PSC was not statistically significant as compared to control on d14 ($p = 0.2$ for both ZT3 and ZT15). Both single agent irinotecan and its combination with PSC inhibited tumor growth at all dose levels and at both administration of ZTs. Maximum tumor growth inhibition occurred on d12, i.e. 4 days after treatment completion. A dose–response relation was found for tumor growth inhibition in mice on single agent irinotecan both at ZT3 and ZT15, with a weak dosing time dependency (Figs. 6a, b and c). Indeed, three-way ANOVA revealed significant effects of dosing time ($p = 0.05$), irinotecan dose level ($p < 0.001$) and an interaction term between irinotecan dose level and PSC addition ($p = 0.02$).

The combination of PSC and irinotecan significantly increased tumor growth inhibition in the mice receiving the lowest irinotecan dose (25 mg/kg/day) at ZT3 resulting in a 70% vs. 28% inhibition. PSC administration at ZT3 even decreased tumor growth inhibition as compared to irinotecan alone at higher doses. In contrast, a consistent dose–response relation was shown in the mice receiving the drug combination at ZT15. Tumor growth inhibition increased from 68% (25 mg/kg/day) to 88% (30 mg/kg/day) and 97% (40 mg/kg/day), yet this latter dose level achieved excessive lethal toxicity (Fig. 6d).

Discussion

Prior studies revealed that single agent irinotecan was best tolerated following dosing in the late light span in male mice (Filipski et al., 2004). Such chronotolerance was coincident with chronoefficacy in male mice bearing GOS treated with single agent irinotecan or the combination of irinotecan and oxaliplatin (Granda et al., 2002). Subsequent experiments indicated a sex-dependent optimal circadian timing for irinotecan chronotolerance (Ahowesso et al., 2011; Li et al., 2013; Okyar et al., 2011).

In the current study, we first searched for a possible relevance of P-gp expression (*Abcb1a* and *Abcb1b*) as a circadian-controlled detoxification mechanism of irinotecan, beside its role in tumor resistance for chemotherapy. The current study was focused on female mice, where the relation between chronotolerance and chronoefficacy was unknown as yet. The mRNA expression of *Abcb1b* was several folds higher than that of *Abcb1a* both in ileum mucosa and in GOS in vivo as well as in vitro. A large amplitude circadian expression was documented for *Abcb1b* but not for *Abcb1a* in ileum mucosa. The highest *Abcb1b* mRNA expression occurred at ZT15, while lowest expression was found at ZT3. In previous work, a circadian rhythm was also documented for *Abcc2* mRNA expression in female B6D2F$_1$ mice, with a maximum at ZT9 and a nadir at ZT0. In this latter study, Abcc2 protein expression was highest at ZT12 and lowest at ZT3 (Okyar et al., 2011). In contrast, despite effective circadian synchronization with dexamethasone (Dibner et al., 2010), no circadian pattern was found for *Abcb1a* or *Abcb1b* in synchronized Per2::Luc GOS cultures. This could result from the continuous proliferation of the cultured Per2::Luc GOS cells. Indeed, a large amplitude circadian rhythm was documented for *ABCB1* in synchronized well differentiated Caco-2 cells at confluence, a condition when minimal proliferation was detected (Ballesta et al., 2011; Lévi et al., 2010).

Here, the administration of single agent irinotecan achieved best tolerability following dosing at ZT15 as compared to ZT3 in female B6D2F$_1$ mice, based on body weight change and hematological toxicities, in good agreement with prior experiments in similar mice (Ahowesso et al., 2011; Li et al., 2013). However, PSC833 alone increased circulating leukocyte counts both at ZT3 and at ZT15. This effect could result from the stimulation of glucocorticoid release by PSC, which in turn produced neutrophil demargination (Cufer et al., 1998; Nakagawa et al., 1998).

No rhythm in tumor P-gp was sought since no circadian expression of clock-controlled genes was found in this tumor model, as a result of molecular clock disruption (Filipski et al., 2005; Iurisci et al., 2006). The P-gp expression in GOS supported a possible therapeutic role for P-gp inhibitors such as PSC in combination with irinotecan.

The current study demonstrated for the first time that PSC administration could disrupt irinotecan chronotolerance and significantly worsen body weight loss, and hematological toxicities. This pharmacologic finding probed that P-gp was an important player in the circadian control of irinotecan detoxification, a mechanism involving increased

efflux of the parent drug and its bioactive metabolite SN-38 (Bansal et al., 2009; Chu et al., 1999; Iyer et al., 2002; Luo et al., 2002). Thus P-gp knock-out mice displayed a 40% decrease in irinotecan biliary excretion. This finding supported its critical role for irinotecan intestinal exposure and its subsequent toxicity for this organ. However, PSC also reduced the biliary transport of SN-38 and SN-38G in P-gp knock-out mice, indicating additional Abcc2 protein inhibition (Iyer et al., 2002). PSC could also compete with irinotecan for CYP3A-mediated metabolism thus reducing its toxicity. However, it was shown that PSC selectively inhibited P-gp rather than CYP3A (Achira et al., 1999). Furthermore, the drug escaped from first-pass liver CYP3A detoxification since it was administered intravenously.

PSC disrupted irinotecan chronotolerance at the highest irinotecan dose (50 mg/kg/day) in non-tumor bearing mice. This could result from inadequate detoxification through joint inhibition of Abcb1a, Abcb1b and Abcc2 protein by PSC. In contrast, no disruption of irinotecan chronotolerance was found following the joint administration of PSC with lower doses of irinotecan (25 and 30 mg/kg/day) in tumor-bearing mice. Furthermore, no worsening of body weight loss was documented on the PSC–irinotecan combination as compared to single agent irinotecan. These results supported adequate irinotecan detoxification at such dose levels. Thus the effect of P-gp inhibition on irinotecan chronotolerance varied according to irinotecan dose level.

Irinotecan doses ranging from 25 to 40 mg/kg/day were significantly more effective at ZT15 as compared to ZT3, both as a single agent or in combination with a fixed dose of PSC, that was selected based upon prior experimental work (Song et al., 1999) and our preliminary experiments. Moreover, PSC consistently increased antitumor efficacy when co-administered with irinotecan at ZT15 only. In contrast, no consistent dose–response was seen in the mice treated at ZT3. PSC administration alone unexpectedly induced tumor progression both at ZT3 and ZT15 but this effect was not statistically significant as compared with vehicle controls. Kankesan et al. (2003, 2004, 2006) revealed that PSC inhibited carcinogen-initiated tumor promotion in rats, yet we found no reported information regarding PSC effects on tumor growth.

The design of optimal therapeutic schedules requires the use of non-toxic doses, i.e. dose levels achieving lethal toxicity in less than ~10% of the tumor-bearing mice. This was the case for both lower doses of irinotecan tested in our study, since a 50% toxic mortality rate was encountered in the mice receiving 40 mg/kg/day of this drug together with PSC. The safest and most effective combination of irinotecan and PSC involved joint treatment at ZT15 and irinotecan doses of 25 or 30 mg/kg/day. This corresponded to a 40 to 50% reduction in the therapeutic dose level of single agent of irinotecan in mice (Filipski et al., 2004; Granda et al., 2002; Li et al., 2013). In this setting, the safest and most effective treatment schedule involved the combination of PSC and irinotecan at a dose level of 30 mg/kg/day at ZT15. This new chronotherapeutic combination schedule increased tumor inhibition by ~40% as compared to single agent irinotecan at the same time and by ~130% as compared to PSC–irinotecan at ZT3. Such chronotherapy optimization resulted from the integration of the differential clock control of P-gp in healthy and tumor tissues.

The ability of PSC to overcome multidrug resistance was tested in 8 randomized trials involving a total of 2276 cancer patients (Boote et al., 1996). These clinical studies planned no systematic reduction of chemotherapy dose levels, nor any circadian timing specification for chemotherapy delivery. None of these studies revealed any benefit from PSC addition to chemotherapy (Baer et al., 2002; Greenberg et al., 2004; Kolitz et al., 2004; Sonneveld et al., 2001; Szakács et al., 2006; van der Holt et al., 2005). Our experimental data support the need for delivering chemotherapy both with a 40% dose reduction and at the circadian time of best tolerability in order to safely improve efficacy with PSC combination. This would correspond to the delivery of irinotecan in the late morning hours in synchronized female patients, i.e. ~3 h after activity onset.

Supporting information and role of the funding source

This study was supported by the ERASysBio + initiative, an EU ERA-NET in FP7, funding the "Circadian and Cell Cycle Clock Systems in Cancer" project (C5Sys); the Association Internationale pour la Recherche sur le Temps Biologique et la Chronotherapie (ARTBC Internationale), Hospital Paul Brousse, Villejuif (France) and the Research Fund of Istanbul University (BAP-7762/2010). None of these sources were involved in the study design, in the collection, analysis and interpretation of data, in the writing of the manuscript, or in the decision to submit the manuscript for publication.

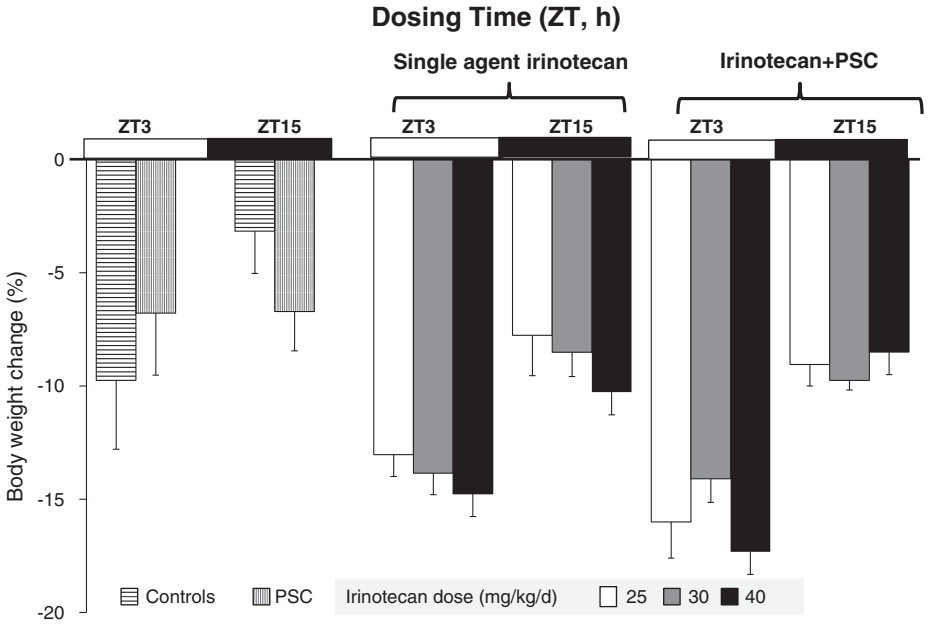

Fig. 5. Time-dependent toxicity of irinotecan as a single agent or combined with PSC in mice. Histogram depicting the dose-dependency of maximum body weight change as a function of dosing time in mice receiving vehicle (control), PSC, or irinotecan as a single agent or in combination with PSC. Body weight change data (mean ± SEM) are expressed relative to pre-treatment values. Note, reduced toxicity following treatment at ZT15 as compared to ZT3 whatever the dose level and irrespective of PSC addition (ANOVA, $p < 0.001$).

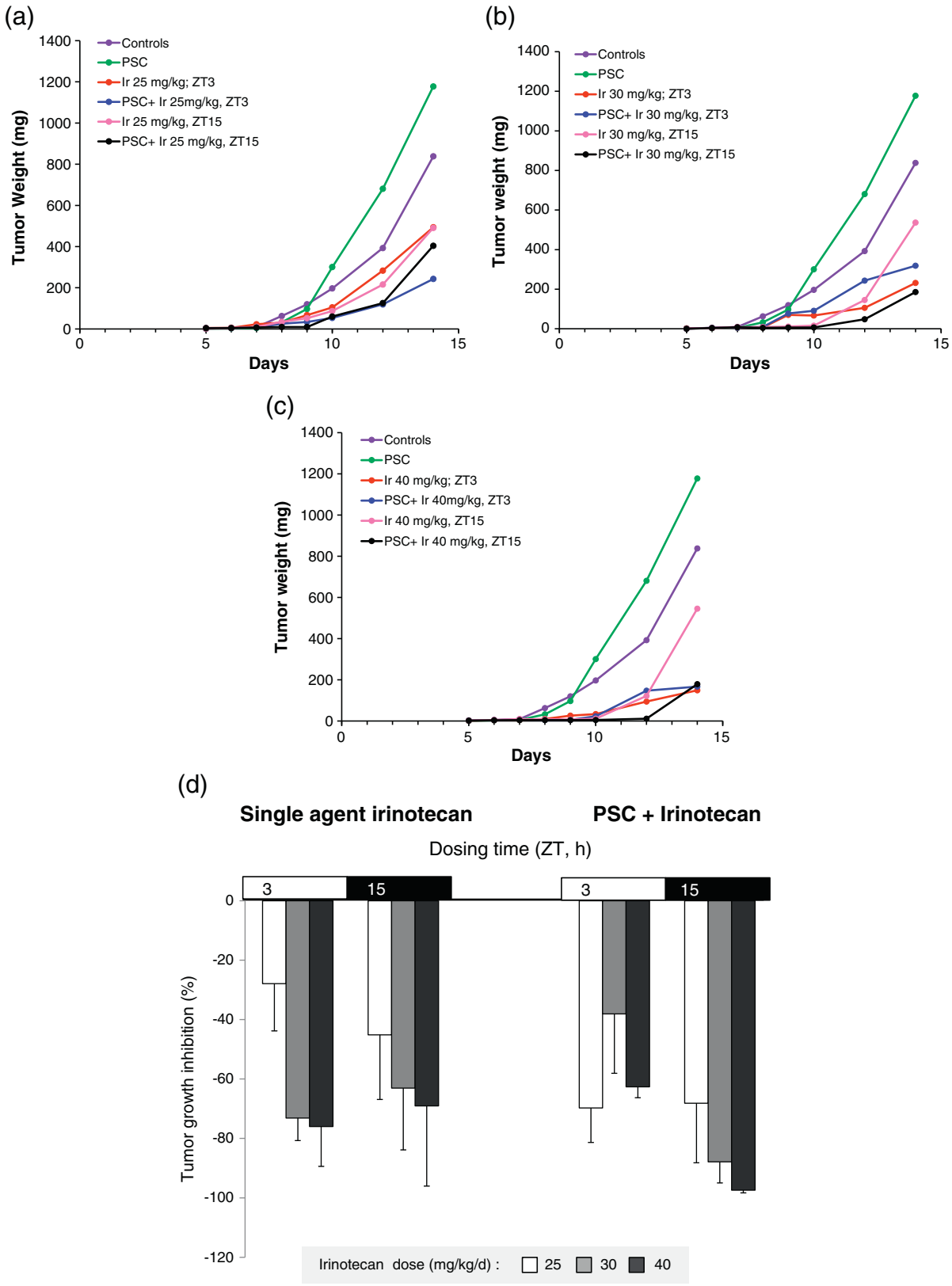

Fig. 6. Circadian time and dose dependency of tumor growth inhibition with irinotecan as a single agent or in combination with PSC. Mean tumor growth curves in controls (pooled data employed) or in mice treated with (a) irinotecan 25 mg/kg/day, (b) 30 mg/kg/day, (c) 40 mg/kg/day; each data point is mean of 6 mice and (d) maximum tumor growth inhibition 4 days after treatment completion (on d12) as a function of irinotecan timing and PSC addition. Data are presented as mean ± SEM. Note the obvious correlation between irinotecan dose and tumor growth inhibition following the administration of single agent irinotecan or its combination with PSC at ZT15 (see text for statistics).

Author contributions

Conceived and designed the experiments: EF, FL, and AO. Performed the experiments: EF, EB, NO, and CG. Analyzed the data: EF, EB, NO, CG, GTJvdH, FL and AO. Wrote the paper: EF, GTJvdH, FL and AO.

Conflict of interest

All authors declare to have no conflict of interest that could have biased the interpretation of the results. The authors alone are responsible for the content and writing of this paper.

Acknowledgments

The authors acknowledge the support of their research by the ERASysBio + initiative, an EU ERA-NET in FP7, funding the "Circadian and Cell Cycle Clock Systems in Cancer" project (C5Sys); and the Association Internationale pour la Recherche sur le Temps Biologique et la Chronotherapie (ARTBC Internationale), Hospital Paul Brousse, Villejuif (France). The research teams of A.O. and F.L. are supported by the Research Fund of Istanbul University (BAP-7762/2010). N.O. is a recipient of a postgraduate fellowship (BIDEB-2214) from the Scientific and Technological Research Council of Turkey (TUBITAK). The authors thank Dr. Peter Krajcsi from SOLVO Company (Budapest-Hungary) for kindly supplying PSC833 and Roel Janssens (Department of Genetics, Erasmus University Medical Center) for his excellent technical assistance.

References

Achira, M., Ito, K., Suzuki, H., Sugiyama, Y., 1999. Comparative studies to determine the selective inhibitors for P-glycoprotein and cytochrome P4503A4. AAPS PharmSci. art 18 1 (4), 1–6.

Ahowesso, C., Li, X.M., Zampera, S., Peteri-Brunbäck, B., Dulong, S., Beau, J., Hossard, V., Filipski, E., Delaunay, F., Claustrat, B., Lévi, F., 2011. Sex and dosing time dependencies in irinotecan-induced circadian disruption. Chronobiol. Int. 28, 458–470.

Ando, H., Yanagihara, H., Sugimoto, K., Hayashi, Y., Tsuruoka, S., Takamura, T., Kaneko, S., Fujimura, A., 2005. Daily rhythms of P-glycoprotein expression in mice. Chronobiol. Int. 22, 655–665.

Baer, M.R., George, S.L., Dodge, R.K., O'Loughlin, K.L., Minderman, H., Caligiuri, M.A., Anastasi, J., Powell, B.L., Kolitz, J.E., Schiffer, C.A., Bloomfield, C.D., Larson, R.A., 2002. Phase III study of the multidrug resistance modulator PSC-833 in previously untreated patients 60 years of age and older with acute myeloid leukemia: Cancer and Leukemia Group B Study 9720. Blood 100, 1224–1232.

Ballesta, A., Dulong, S., Abbara, C., Cohen, B., Okyar, A., Clairambault, J., Lévi, F., 2011. A combined experimental and mathematical approach for molecular-based optimization of irinotecan circadian delivery. PLoS Comput. Biol. 7 (9), e1002143. http://dx.doi.org/10.1371/journal.pcbi.1002143.

Bansal, T., Mishra, G., Jaggi, M., Khar, R.K., Talegaonkar, S., 2009. Effect of P-glycoprotein inhibitor, verapamil, on oral bioavailability and pharmacokinetics of irinotecan in rats. Eur. J. Pharm. Sci. 36, 580–590.

Bissery, M.C., Vrignaud, P., Lavelle, F., Chabot, G.G., 1996. Experimental antitumor activity and pharmacokinetics of the camptothecin analog irinotecan (CPT-11) in mice. Anticancer Drugs 7, 437–460.

Boote, D.J., Dennis, I.F., Twentyman, P.R., Osborne, R.J., Laburte, C., Hensel, S., Smyth, J.F., Brampton, M.H., Bleehen, N.M., 1996. Phase I study of etoposide with SDZ PSC 833 as a modulator of multidrug resistance in patients with cancer. J. Clin. Oncol. 14, 610–618.

Cagliero, E., Ferracini, R., Morello, E., Scotlandi, K., Manara, M.C., Buracco, P., Comandone, A., Baroetto-Paris, R., Baldini, N., 2004. Reversal of multidrug-resistance using valspodar (PSC 833) and doxorubicin in osteosarcoma. Oncol. Rep. 12, 1023–1031.

Chomczynski, P., Sacchi, N., 2006. The single-step method of RNA isolation by acid guanidinium thiocyanate–phenol–chloroform extraction: twenty-something years on. Nat. Protoc. 1, 581–585.

Chu, X.Y., Kato, Y., Sugiyama, Y., 1999. Possible involvement of P-glycoprotein in biliary excretion of CPT-11 in rats. Drug Metab. Dispos. 27, 440–441.

Claudel, T., Cretenet, G., Saumet, A., Gachon, F., 2007. Crosstalk between xenobiotics metabolism and circadian clock. FEBS Lett. 581, 3626–3633.

Cufer, T., Vrhovec, I., Pfeifer, M., Skrk, J., Borstnar, S., Sikic, B., 1998. Effect of the multidrug resistance modulator valspodar on serum cortisol levels in rabbits. Cancer Chemother. Pharmacol. 41, 517–521.

De Prins, J., Hecquet, B., 1992. In: Touitou, Y., Haus, E. (Eds.), Biological Rhythms in Clinical and Laboratory Medicine. Springer Verlag, Berlin, pp. 90–112.

Dibner, C., Schibler, U., Albrecht, U., 2010. The mammalian circadian timing system: organization and coordination of central and peripheral clock. Annu. Rev. Physiol. 72, 517–549.

Filipski, E., Lemaigre, G., Liu, X.H., Mery-Mignard, D., Mahjoubi, M., Lévi, F., 2004. Circadian rhythm of irinotecan tolerability in mice. Chronobiol. Int. 21, 613–630.

Filipski, E., Innominato, P.F., Wu, M., Li, X.M., Iacobelli, S., Xian, L.J., Lévi, F., 2005. Effects of light and food schedules on liver and tumor molecular clocks in mice. J. Natl. Cancer Inst. 97, 507–517.

Gachon, F., Olela, F.F., Schaad, O., Descombes, P., Schibler, U., 2006. The circadian PAR domain basic leucine zipper transcription factors DBP, TEF, and HLF modulate basal and inducible xenobiotic detoxification. Cell Metab. 4, 25–36.

Giacchetti, S., Dugué, P.A., Innominato, P.F., Bjarnason, G.A., Focan, C., Garufi, C., Tumolo, S., Coudert, B., Iacobelli, S., Smaaland, R., Tampellini, M., Adam, R., Moreau, T., Lévi, F., 2012. Sex moderates circadian chemotherapy effects on survival of patients with metastatic colorectal cancer: a meta-analysis. Ann. Oncol. 23, 3110–3116.

Granda, T.G., D'Attino, R.M., Filipski, E., Vrignaud, P., Garufi, C., Terzoli, E., Bissery, M.C., Lévi, F., 2002. Circadian optimisation of irinotecan and oxaliplatin efficacy in mice with Glasgow osteosarcoma. Br. J. Cancer 86, 999–1005.

Greenberg, P.L., Lee, S.J., Advani, R., Tallman, M.S., Sikic, B.I., Letendre, L., Dugan, K., Lum, B., Chin, D.L., Dewald, G., Paietta, E., Bennett, J.M., Rowe, J.M., 2004. Mitoxantrone, etoposide and cytarabine with or without valspodar in patients with relapsed or refractory acute myelod leukemia and high-risk myelodysplastic syndrome: a phase III trial (E2995). J. Clin. Oncol. 22, 1078–1086.

Innocenti, F., Ratain, M.J., 2003. Irinotecan treatment in cancer patients with UGT1A1 polymorphisms. Oncology (Williston Park) 17 (Suppl. 5), 52–55.

Iurisci, I., Filipski, E., Reinhardt, J., Bach, S., Gianella-Borradori, A., Iacobelli, S., Meijer, L., Lévi, F., 2006. Improved tumor control through circadian clock induction by Seliciclib, a cyclin-dependent kinase inhibitor. Cancer Res. 66, 10720–11028.

Iyer, L., Ramírez, J., Shepard, D.R., Bingham, C.M., Hossfeld, D.K., Ratain, M.J., Mayer, U., 2002. Biliary transport of irinotecan and metabolites in normal and P-glycoprotein-deficient mice. Cancer Chemother. Pharmacol. 49, 336–341.

Johnson, B.M., Charman, W.N., Porter, C.J., 2003. Application of compartmental modeling to an examination of in vitro intestinal permeability data: assessing the impact of tissue uptake, P-glycoprotein, and CYP3A. Drug Metab. Dispos. 31, 1151–1160.

Kankesan, J., Yusuf, A., Laconi, E., Vanama, R., Bradley, G., Thiessen, J., Ling, V., Rao, P., Rajalakshmi, S., Sarma, D.S.R., 2003. Effect of PSC833, an inhibitor of P-glycoprotein, on 1,2-dimethylhydrazine-induced liver carcinogenesis in rats. Carcinogenesis 24, 1977–1984.

Kankesan, J., Vanama, R., Yusuf, A., Thiessen, J., Ling, V., Rao, P., Rajalakshmi, S., Sarma, D.S.R., 2004. Effect of PSC833, an inhibitor of P-glycoprotein on N-methyl-N-nitrosourea induced mammary carcinogenesis in rats. Carcinogenesis 25, 425–430.

Kankesan, J., Laconi, E., Medline, A., Thiessen, J., Ling, V., Rao, P.M., Rajalakshmi, S., Sarma, D.S.R., 2006. PSC833, an inhibitor of P-glycoprotein inhibits 1,2-dimethylhydrazine-induced colorectal carcinogenesis in male Fischer F344 rats. Anticancer Res. 26, 995–999.

Kemper, E.M., van Zandbergen, A.E., Cleypool, C., Mos, H.A., Boogerd, W., Beijnen, J.H., van Tellingen, O., 2003. Increased penetration of paclitaxel into the brain by inhibition of P-glycoprotein. Clin. Cancer Res. 9, 2849–2855.

Kolitz, J.E., George, S.L., Dodge, R.K., Hurd, D.D., Powell, B.L., Allen, S.L., Velez-Garcia, E., Moore, J.O., Shea, T.C., Hoke, E., Caligiuri, M.A., Vardiman, J.W., Bloomfield, C.D., Larson, R.A., 2004. Dose escalation studies of cytarabine, daunorubicin, and etoposide with and without multidrug resistance modulation with PSC-833 in untreated adults with acute myeloid leukemia younger than 60 years: final induction results of Cancer and Leukemia Group B Study 9621. J. Clin. Oncol. 22, 4290–4301.

Krishna, R., Mayer, L.D., 1999. The use of liposomal anticancer agents to determine the roles of drug pharmacodistribution and P-glycoprotein (PGP) blockade in overcoming multidrug resistance (MDR). Anticancer Res. 19 (4B), 2885–2891.

Lévi, F., 2006. Chronotherapeutics: the relevance of timing in cancer therapy. Cancer Causes Control 17, 611–621.

Lévi, F., Okyar, A., 2011. Circadian clocks and drug delivery systems: impact and opportunities in chronotherapeutics. Expert Opin. Drug Deliv. 8, 1535–1541.

Lévi, F., Schibler, U., 2007. Circadian rhythms: mechanisms and therapeutic implications. Annu. Rev. Pharmacol. Toxicol. 47, 593–628.

Lévi, F., Zidani, R., Misset, J.L., 1997. Randomized multicenter trial of chronotherapy with oxaliplatin, 5-fluorouracil, and folinic acid in metastatic colorectal cancer. Lancet 350, 681–686.

Lévi, F., Focan, C., Karaboué, A., de la Valette, V., Focan-Henrard, D., Baron, B., Kreutz, F., Giacchetti, S., 2007. Implications of circadian clocks for the rhythmic delivery of cancer therapeutics. Adv. Drug Deliv. Rev. 59, 1015–1035.

Lévi, F., Altinok, A., Clairambault, J., Goldbeter, A., 2008. Implications of circadian clocks for the rhythmic delivery of cancer therapeutics. Philos. Trans. R. Soc. A 366, 3575–3598.

Lévi, F., Okyar, A., Dulong, S., Innominato, P.F., Clairambault, J., 2010. Circadian timing in cancer treatment. Annu. Rev. Pharmacol. Toxicol. 50, 377–410.

Li, X.M., Mohammad-Djafari, A., Dumitru, M., Dulong, S., Filipski, E., Siffroi-Fernandez, S., Mteyrek, A., Scaglione, F., Guettier, C., Delaunay, F., Lévi, F., 2013. A circadian clock transcription model for the personalization of cancer chronotherapy. Cancer Res. 73 (24). http://dx.doi.org/10.1158/0008-5472.CAN-13-1528 (Epub ahead of print).

Luo, F.R., Paranjpe, P.V., Guo, A., Rubin, E., Sinko, P., 2002. Intestinal transport of irinotecan in Caco-2 cells and MDCK II cells overexpressing efflux transporters Pgp, cMOAT, and MRP1. Drug Metab. Dispos. 30 (7), 763–770.

Murakami, Y., Higashi, Y., Matsunaga, N., Koyanagi, S., Ohdo, S., 2008. Circadian clock controlled intestinal expression of the multidrug-resistance gene mdr1a in mice. Gastroenterology 135, 1636–1644.

Nakagawa, M., Terashima, T., D'yachkova, Y., Bondy, G., Hogg, J., van Eeden, S., 1998. Glucocorticoid-induced granulocytosis: contribution of marrow release and demargination of intravascular granulocytes. Circulation 98, 2307–2313.

Ohdo, S., Makinosumi, T., Ishizaki, T., Yukawa, E., Higuchi, S., Nakano, S., Ogawa, N., 1997. Cell cycle-dependent chronotoxicity of irinotecan hydrochloride in mice. J. Pharmacol. Exp. Ther. 283, 1383–1388.

Okyar, A., Piccolo, E., Ahowesso, C., Filipski, E., Hossard, V., Guettier, C., La Sorda, R., Tinari, N., Iacobelli, S., Lévi, F., 2011. Strain- and sex-dependent circadian changes in abcc2 transporter expression: implications for irinotecan chronotolerance in mouse ileum. PLoS One. http://dx.doi.org/10.1371/journal.pone.0020393.

Okyar, A., Dressler, C., Hanafy, A., Baktir, G., Lemmer, B., Spahn-Langguth, H., 2012. Circadian variations in exsorptive transport: in situ intestinal perfusion data and in vivo relevance. Chronobiol. Int. 29 (4), 443–453.

Page, R.L., Hughes, C.S., Huyan, S., Sagris, J., Trogdon, M., 2000. Modulation of P-glycoprotein-mediated doxorubicin resistance in canine cell lines. Anticancer Res. 20 (5B), 3533–3538.

Song, S., Suzuki, H., Kawai, R., Sugiyama, Y., 1999. Effect of PSC 833, a P-glycoprotein modulator, on the disposition of vincristine and digoxin in rats. Drug Metab. Dispos. 27, 689–694.

Sonneveld, P., Sauci, S., Weijermans, P., Beksac, M., Neuwirtova, R., Solbu, G., Lokhorst, H., van der Lelie, J., Dohner, H., Gerhartz, H., Segeren, C.M., Willemze, R., Lowenberg, B., 2001. Cyclosporine A combined with vincristine, doxorubicine and dexamethasone (VAD) compared with VAD alone in patients with advanced refractory multiple myeloma. Br. J. Haematol. 115, 895–902.

Szakács, G., Paterson, J.K., Ludwig, J.A., Booth-Genthe, C., Gottesmann, M.M., 2006. Targeting multidrug resistance in cancer. Nat. Rev. Drug Discov. 3, 219–234.

Tai, H.L., 2000. Technology evaluation: Valspodar, Novartis AG. Curr. Opin. Mol. Ther. 2, 459–467.

Tampellini, M., Filipski, E., Liu, X.H., Lemaigre, G., Li, X.M., Vrignaud, P., François, E., Bissery, M.C., Lévi, F., 1998. Docetaxel chronopharmacology in mice. Cancer Res. 58, 3896–3904.

van der Holt, B., Löwenberg, B., Burnett, A.K., Knauf, W.U., Shepherd, J., Piccaluga, P.P., Ossenkoppele, G.J., Verhoef, G.E., Ferrant, A., Crump, M., Selleslag, D., Theobald, M., Fey, M.F., Vellenga, E., Dugan, M., Sonneveld, P., 2005. The value of the MDR1 reversal agent PSC-833 in addition to daunorubicin and cytarabine in the treatment of elderly patients with previously untreated acute myeloid leukemia (AML), in relation to MDR1 status at diagnosis. Blood 106 (8), 2646–2654.

Watanabe, T., Tsuge, H., Oh-Hara, T., Naito, M., Tsuruo, T., 1995. Comparative study on reversal efficacy of SDZ PSC 833, cyclosporin A and verapamil on multidrug resistance in vitro and in vivo. Acta Oncol. 34, 235–241.

Zhang, Y.K., Yeager, R.L., Klaassen, C.D., 2009. Circadian expression profiles of drug-processing genes and transcription factors in mouse liver. Drug Metab. Dispos. 3, 106–115.